INTERNATIONAL JOURNAL FOR NUMERICAL METHODS IN FLUIDS
Int. J. Numer. Meth. Fluids 2007; **54**:393–417
Published online 12 December 2006 in Wiley InterScience (www.interscience.wiley.com). DOI: 10.1002/fld.1404

Numerical study of wave propagation in compressible two-phase flow

D. Zeidan[1], E. Romenski[2], A. Slaouti[3,*,†] and E. F. Toro[2]

[1]*Department of Basic Sciences, Al-Balqa Applied University, Al-Salt, Jordan*
[2]*Laboratory of Applied Mathematics, University of Trento, Trento, Italy*
[3]*Department of Engineering and Technology, Manchester Metropolitan University, Manchester, U.K.*

SUMMARY

We propose a new model and a solution method for two-phase two-fluid compressible flows. The model involves six equations obtained from conservation principles applied to a one-dimensional flow of gas and liquid mixture completed by additional closure governing equations. The model is valid for pure fluids as well as for fluid mixtures. The system of partial differential equations with source terms is hyperbolic and has conservative form. Hyperbolicity is obtained using the principles of extended thermodynamics. Features of the model include the existence of real eigenvalues and a complete set of independent eigenvectors. Its numerical solution poses several difficulties. The model possesses a large number of acoustic and convective waves and it is not easy to upwind all of these accurately and simply. In this paper we use relatively modern shock-capturing methods of a centred-type such as the total variation diminishing (TVD) slope limiter centre (SLIC) scheme which solve these problems in a simple way and with good accuracy. Several numerical test problems are displayed in order to highlight the efficiency of the study we propose. The scheme provides reliable results, is able to compute strong shock waves and deals with complex equations of state. Copyright © 2006 John Wiley & Sons, Ltd.

Received 4 June 2004; Revised 2 October 2006; Accepted 15 October 2006

KEY WORDS: compressible two-phase flow; extended thermodynamics; hyperbolic conservative two-fluid model; TVD centred schemes

1. INTRODUCTION

This paper is concerned with the numerical study for solving a system of balance laws modelling one-dimensional compressible two-phase flow. The ability to efficiently evaluate two-phase flow

*Correspondence to: A. Slaouti, Department of Engineering and Technology, Manchester Metropolitan University, Manchester, U.K.
†E-mail: a.slaouti@mmu.ac.uk

Contract/grant sponsor: EU Commission; contract/grant number: FIKS-CT-2000-00050

phenomena is needed to understand many processes of practical concern. For instance, nuclear reactor safety studies and pressure relief capabilities of many chemical reactors require this ability. In general, the ability to predict these phenomena depends on the availability of valid mathematical models and robust numerical methods. This is a very challenging task, as the numerical methods must combine robustness and accuracy and cover a wide domain of physical conditions, including the whole range of void fraction from single to mixture two-phase flow regime, and a wide range of pressure conditions. Numerical methods [1–3] on which current generation of two-phase flow codes used in industry is based are certainly robust but are known to suffer from excessive numerical dissipation. This in turns limits our ability to improve physical modelling and generally our understanding of compressible two-phase flow processes. A two-phase flow problem can be formulated by using a two-fluid model, depending on the degree of the dynamic coupling between the phases. Early two-fluid models did not result in a system of hyperbolic equations [4–7]. Such models used in practice with a degree of success lead to ill-posed initial-value problem and hence are physically unacceptable. In order to make these models hyperbolic, some researchers introduce formulations for coupling the two separated momentum equations, including space and time derivatives of physical quantities (virtual mass term, interfacial pressure, see [8–18]). Thus, the correct formulation of the basic two-fluid equations and the appropriate closure relations have been discussed during the past and, up to now, there does not exist a commonly agreed approach. Two-phase flows always involve some relative motion of one phase with respect to the other. Therefore, a two-phase flow problem can be formulated phenomenologically in terms of two velocity fields [19–21]. The difficulties associated with the two-fluid model are greatly reduced by formulating a two-phase problem in terms of extended thermodynamics which provides reliable results for modelling complicated media with rapidly varying and strongly inhomogeneous processes [22–25]. The resulting model is a conservative first-order quasi-linear symmetric hyperbolic system of field equations and allows discontinuous solutions [26–29]. Crucial new aspects of this hyperbolic conservative model of two-phase flow are the existence of real eigenvalues and a corresponding set of linearly independent eigenvectors. This allows the application of modern numerical schemes [30] which make use of the hyperbolicity of the flow equations.

Progress in numerical modelling of two-phase flow has been slower than for single-phase flow, for which the last two decades have seen the development and maturity of high resolution numerical schemes such as Godunov-type methods and efficient unstructured mesh techniques. It was in the late 1980s and beginning of the 1990s that these advanced numerical methods were considered for the modelling of various types of two-phase flow, in sectors ranging from solid combustion [31–35] to nuclear reactor safety thermal-hydraulics [36–40] to oil transport [41–44]. In the past few years, a number of shock-capturing schemes have been constructed to solve systems of conservation laws [45–52]. These methods are characterized as being of first-order or by their higher accuracy in the smooth regions of the solution without presenting the spurious oscillations associated with the conventional second-order schemes in the presence of discontinuities. Toro in [53] introduced the centred total variation diminishing (TVD) methods which have the property that they are second-order accurate and may be oscillation-free across discontinuities. Centred methods are methods that do not require the explicit solution of the Riemann problem, i.e. they are not based by the wave propagation direction. This feature is especially used for typical problems, arising in two-phase flow modelling, where we often have to complete the equation model by extra equations. These could be the balance equations for the gas volume and mass concentrations, and the relative velocity balance law. Such types of systems involve more equations, but remain hyperbolic and have the same structure. In this paper we describe a general method to the modern TVD scheme

DOI: 10.1002/fld

introduced by Toro [53] to hyperbolic conservation laws modelling compressible two-phase flow, giving rise to a set of sufficient condition which are useful in checking or constructing second-order TVD schemes. We propose to use slope limiter centre (SLIC) scheme. We emphasize that the SLIC scheme has never been used to solve these models. The SLIC scheme is suitable for very complicated problems for which the Riemann problem solution is unavailable or too complicated as in the hyperbolic conservative two-fluid model case. This scheme uses three steps: (I) data reconstruction, (II) evolution and (III) the Riemann problem. In our implementation, the evolution step employs the solution of the Riemann problem to evaluate the first-order centred (FORCE) flux of the hyperbolic conservative two-fluid model. The rest of this paper is organized as follows. In Section 2 we present the two-phase flow model to which numerical study is considered, and we look at the hyperbolicity of the model. The next section is devoted to the construction of the numerical approach to the hyperbolic conservative two-fluid model. Following the method developed in [53] for conservation laws, we describe SLIC scheme. Finally, the application of the described scheme to solve the two-phase flow problems is explained and numerical results are presented in the last section. These results include examples for typical two-phase flow problems, which confirm that the model gives excellent results. Clearly, a more detailed study of the mathematical and numerical character of the two-phase flow equations are warranted and future studies may lead to better understanding of the coupling of the various modes of two-phase flows.

Further details about the description, analysis and application of the model and the numerical scheme described in this paper are presented in the PhD thesis of the first author [54].

2. TWO-PHASE FLOW-HYPERBOLIC CONSERVATIVE MODEL

Two-phase flow models have applications within several areas and are known for being quite complicated both from a modelling and numerical point of view. Following Romenski [25], one-dimensional two-phase flow with different phase velocities can be described by a conservative two-fluid model six first order non-linear partial differential equations describing mass, momentum and energy conservation for the mixture, a balance law for the volume concentration of the second phase, a balance law for mass concentration of the second phase and a balance law for the relative velocity between the two phases. The dynamics of two-phase flow is determined by these balance equations which involve source terms for interphase exchanges of volume concentration and relative velocity between phases. In addition, the relaxation of volume concentration to equilibrium state and interfacial friction are chiefly responsible for the development of the flow.

The two-fluid model is widely used within the chemical reactors and it is well known that modelling of flows involving mixtures is a difficult task. Another area of application for two-phase fluid flows concerns, for example, safety of nuclear reactors which is an area of great importance for the industrial field. Considering two-phase flow in the nuclear industry, it is convenient to identify a class of physical phenomena such as pressure wave propagation through a gas and liquid flow. Pressure wave propagation study is useful for safety reasons, for flow regulation and providing information about flow properties. Further knowledge about pressure propagation can aid in flow control because a change in flow rate or pressure at the inlet or outlet generates a pressure wave. From a numerical point of view, the correct description of pressure waves require high-order schemes possessing little numerical diffusion. In addition, it is important for the industry that the schemes can produce solutions within a reasonable range of accuracy and time.

DOI: 10.1002/fld

The focus of this work is the numerical aspects: we will limit ourselves to consider a mixture of two-phase gas and liquid flow. The effects of viscosity are assumed to be absent while there is no mass transfer between the phases. The one-dimensional hyperbolic conservative model then takes the following form [54]:

The mixture mass conservation equation is

$$\partial_t(\rho) + \partial_x(\rho u) = 0 \tag{1}$$

The mixture momentum conservation equation is

$$\partial_t(\rho u) + \partial_x(\rho u^2 + \mathscr{P} + \rho u_\mathrm{r}\mathscr{E}_{u_\mathrm{r}}) = 0 \tag{2}$$

The mixture energy conservation equation is given by

$$\partial_t\left(\rho\left(\mathscr{E} + \frac{u^2}{2}\right)\right) + \partial_x\left(\rho u\left(\mathscr{E} + \frac{u^2}{2}\right) + \mathscr{P}u + \rho u u_\mathrm{r}\mathscr{E}_{u_\mathrm{r}} + \rho\mathscr{E}_\mathrm{c}\mathscr{E}_{u_\mathrm{r}}\right) = 0 \tag{3}$$

In (1)–(3), t is the time, x is the flow direction (spacial coordinate), α is the volume fraction of the gas phase, $\rho = (1-\alpha)\rho_1 + \alpha\rho_2$ is the mixture density, $\rho u = (1-\alpha)\rho_1 u_1 + \alpha\rho_2 u_2$ is the mixture momentum and the subscripts 1 and 2 refer to the liquid and gas phases, respectively. The conserved quantities in (1)–(3) represent the mixture mass, mixture momentum and mixture energy. In addition, several closure laws must be given which involve the gas volume concentration balance law, the mass gas concentration conservation law and the relative velocity balance law.

The gas volume concentration balance law is

$$\partial_t(\rho\alpha) + \partial_x(\rho u\alpha) = \phi \tag{4}$$

The source term ϕ is found to be

$$\phi = -\frac{\rho}{\tau}\mathscr{E}_\alpha \tag{5}$$

which describe the relaxation of volume concentration to equilibrium state with relaxation time τ (which can be a function of parameters of state).

The mass gas concentration conservation law is

$$\partial_t(\rho c) + \partial_x(\rho u c + \rho\mathscr{E}_{u_\mathrm{r}}) = 0 \tag{6}$$

Finally, the relative velocity balance law is

$$\partial_t(u_\mathrm{r}) + \partial_x(u u_\mathrm{r} + \mathscr{E}_\mathrm{c}) = \pi \tag{7}$$

where the source term π is the interfacial friction defined as

$$\pi = -\kappa c(1-c)u_\mathrm{r} \tag{8}$$

where κ can depend on the parameters of state.

To close system (1)–(3) and (4)–(7) we define the pressure as

$$\mathscr{P} = \rho^2\mathscr{E}_\rho \tag{9}$$

DOI: 10.1002/fld

and the mixture internal energy (EOS) as

$$\mathscr{E}(\rho, \alpha, c, u_{\mathrm{r}}, \mathscr{S}) = \mathfrak{e}(\rho, \alpha, c, \mathscr{S}) + c(1-c)\frac{u_{\mathrm{r}}u_{\mathrm{r}}}{2} \tag{10}$$

which is determined by the equations of state for the air and water [54].

Now if we let

$$\mathbb{U} = \begin{pmatrix} \rho \\ \rho\alpha \\ \rho u \\ \rho c \\ u_{\mathrm{r}} \\ \rho\left(\mathscr{E} + \dfrac{u^2}{2}\right) \end{pmatrix}, \quad \mathbb{F}(\mathbb{U}) = \begin{pmatrix} \rho u \\ \rho u\alpha \\ \rho u^2 + \mathscr{P} + \rho u_{\mathrm{r}}\mathscr{E}_{u_{\mathrm{r}}} \\ \rho uc + \rho\mathscr{E}_{u_{\mathrm{r}}} \\ uu_{\mathrm{r}} + \mathscr{E}_{\mathrm{c}} \\ \rho u\left(\mathscr{E} + \dfrac{u^2}{2}\right) + \mathscr{P}u + \rho uu_{\mathrm{r}}\mathscr{E}_{u_{\mathrm{r}}} + \rho\mathscr{E}_{\mathrm{c}}\mathscr{E}_{u_{\mathrm{r}}} \end{pmatrix} \tag{11}$$

and

$$\mathbb{S}(\mathbb{U}) = [0, \phi, 0, 0, \pi, 0]^{\mathrm{T}} \tag{12}$$

then (1)–(3) and (4)–(7) can be written as a 6×6 system of conservation laws

$$\partial_t\mathbb{U} + \partial_x\mathbb{F}(\mathbb{U}) = \mathbb{S}(\mathbb{U}), \quad -\infty < x < \infty, \quad t > 0 \tag{13}$$

Letting J denote the Jacobian matrix of $\mathbb{F}$ with respect to the conservative variables $\mathbb{U}$, we can write

$$\partial_t\mathbb{U} + J\partial_x(\mathbb{U}) = \mathbb{S}(\mathbb{U}) \tag{14}$$

Generally, it is difficult to express the flux function $\mathbb{F}$ in terms of conservative variables. From a physical point of view, the vector of conservative variables $\mathbb{U}$ is not a convenient state vector with which to work. The closure laws are formulated in terms of physical variables (primitive variables). Also, from a numerical point of view, numerical schemes based on conservative variables will require some iterative procedure to transform these variables into primitive variables for each calculation. This leads us to consider other alternatives based on primitive formulations. For the one-dimensional conservative two-fluid model, one possible primitive formulation is the vector $\mathbb{W}$ defined as

$$\mathbb{W} = [\rho, \alpha, u, c, u_{\mathrm{r}}, \mathscr{S}]^{\mathrm{T}} \tag{15}$$

Thus, in quasi-linear form we have [54]

$$\partial_t\mathbb{W} + \mathbb{A}(\mathbb{W})\partial_x\mathbb{W} = \bar{\mathbb{S}}(\mathbb{W}) \tag{16}$$

DOI: 10.1002/fld

where the matrix $\mathbb{A}(\mathbb{W})$ is

$$\begin{pmatrix} u & 0 & \rho & 0 & 0 & 0 \\ 0 & u & 0 & 0 & 0 & 0 \\ \dfrac{1}{\rho}(\mathscr{P}_\rho + c(1-c)u_\mathrm{r}^2) & \dfrac{\mathscr{P}_\alpha}{\rho} & u & \dfrac{1}{\rho}(\mathscr{P}_\mathrm{c} + \rho(1-2c)u_\mathrm{r}^2) & 2c(1-c)u_\mathrm{r} & \dfrac{\mathscr{P}_\mathscr{S}}{\rho} \\ c(1-c)\dfrac{u_\mathrm{r}}{\rho} & 0 & 0 & u+(1-2c)u_\mathrm{r} & c(1-c) & 0 \\ \mathrm{e}_{\mathrm{c}\rho} & \mathrm{e}_{\alpha\mathrm{c}} & u_\mathrm{r} & \mathrm{e}_{\mathrm{cc}} - u_\mathrm{r}^2 & u+(1-2c)u_\mathrm{r} & \mathrm{e}_{c\mathscr{S}} \\ 0 & 0 & 0 & 0 & 0 & u \end{pmatrix} \tag{17}$$

and the source terms are

$$\bar{\mathbb{S}}(\mathbb{W}) = \left[0, \frac{\phi}{\rho}, 0, 0, \pi, \Lambda\right]^\mathrm{T} \tag{18}$$

where

$$\Lambda = -\frac{1}{\mathscr{E}_\rho}(\mathscr{E}_\alpha \phi + \mathscr{E}_{u_\mathrm{r}} \pi) \geqslant 0$$

is the entropy production.

Before discussing the numerical aspects, we need to study the mathematical properties of the model. We begin with the hyperbolicity of the model in processes without dissipation, i.e.

$$\partial_t \mathbb{U} + \partial_x \mathbb{F}(\mathbb{U}) = 0, \quad -\infty < x < \infty, \quad t > 0 \tag{19}$$

Let us introduce the set Ω of physically admissible states, $\Omega = \{\mathbb{U} \in \mathbb{R}^6;\ \rho > 0, \mathscr{S} > 0, \alpha, c \in]0, 1[, u, u_\mathrm{r} \in \mathbb{R}\}$ and denote the speed of sound for the mixture two-phase flow by a. Then we can find a positive number $u_\mathrm{r}^\star$ such that for any $\mathbb{U}$ that lies in the set $\Omega^\star$ defined by $\Omega^\star = \{\mathbb{U} \in \Omega;\ |u_\mathrm{r}| \leqslant u_\mathrm{r}^\star\}$ and the eigenvalues λ_j, $1 \leqslant \mathrm{j} \leqslant 6$ are real and for u_r small enough given by [54]

$$\lambda_1 = u - a_1 + \mathscr{Y}(a_1)u_\mathrm{r} + \mathscr{O}(u_\mathrm{r}^2) \tag{20}$$

$$\lambda_2 = u - a_2 + \mathscr{Y}(a_2)u_\mathrm{r} + \mathscr{O}(u_\mathrm{r}^2) \tag{21}$$

$$\lambda_3 = \lambda_4 = u \tag{22}$$

$$\lambda_5 = u + a_1 + \mathscr{Y}(a_1)u_\mathrm{r} + \mathscr{O}(u_\mathrm{r}^2) \tag{23}$$

$$\lambda_6 = u + a_2 + \mathscr{Y}(a_2)u_\mathrm{r} + \mathscr{O}(u_\mathrm{r}^2) \tag{24}$$

where

$$a_1 = \frac{1}{\sqrt{2}}\left[-\varsigma_2^0 + \sqrt{(\varsigma_2^0)^2 - 4\varsigma_0^0}\right]^{1/2}$$

$$a_2 = \frac{1}{\sqrt{2}}\left[-\varsigma_2^0 - \sqrt{(\varsigma_2^0)^2 - 4\varsigma_0^0}\right]^{1/2}$$

DOI: 10.1002/fld

and

$$\mathscr{Y}(a_{\mathrm{i}}) = \frac{\varsigma_1^1 + \varsigma_3^1 a_{\mathrm{i}}^2}{2(\varsigma_2^0 + 2a_{\mathrm{i}}^2)}, \quad \mathrm{i} = 1, 2$$

with

$$\begin{aligned}
\varsigma_3^1 &= 2(1-2c)\\
\varsigma_2^0 &= -(\mathscr{P}_\rho + c(1-c)\mathrm{e}_{\mathrm{cc}})\\
\varsigma_1^1 &= 2(2\rho c(1-c)\mathrm{e}_{\mathrm{c}\rho} - (1-2c)\mathscr{P}_\rho)\\
\varsigma_0^0 &= c(1-c)(\mathscr{P}_\rho \mathrm{e}_{\mathrm{cc}} - \mathscr{P}_{\mathrm{c}}\mathrm{e}_{\mathrm{c}\rho})
\end{aligned}$$

Moreover, the corresponding eigenvectors of system (19) in the system of variables $\mathbb{W}$ can be chosen as

$$\mathscr{K}^{\pm}(\mathbb{W}) = k \begin{pmatrix} 1 \\ \vartheta_0 + \vartheta_1 u_{\mathrm{r}} \\ \vartheta_2 + \vartheta_3 u_{\mathrm{r}} \\ \vartheta_4 + \vartheta_5 u_{\mathrm{r}} \end{pmatrix} \tag{25}$$

$$\mathscr{K}^{0-}(\mathbb{W}) = \begin{pmatrix} 0 \\ 1 \end{pmatrix}, \quad \mathscr{K}^{0+}(\mathbb{W}) = \begin{pmatrix} 1 \\ 0 \end{pmatrix} \tag{26}$$

where

$$\vartheta_0 = \pm\frac{a_{1,2}}{\rho}, \quad \vartheta_1 = -\frac{\mathscr{Y}}{\rho}, \quad \vartheta_2 = -\frac{c(1-c)\mathrm{e}_{\mathrm{c}\rho}}{c(1-c)\mathrm{e}_{\mathrm{cc}} - a_{1,2}^2}$$

$$\vartheta_3 = \pm\frac{2a_{1,2}((1-2c)+\mathscr{Y})}{c(1-c)\mathrm{e}_{\mathrm{cc}} - a_{1,2}^2}, \quad \vartheta_4 = \pm\frac{\mathrm{e}_{\mathrm{c}\rho}}{a_{1,2}} \pm \frac{c(1-c)\mathrm{e}_{\mathrm{c}\rho}\mathrm{e}_{\mathrm{cc}}}{a_{1,2}[c(1-c)\mathrm{e}_{\mathrm{cc}} - a_{1,2}^2]}$$

$$\vartheta_5 = \frac{1}{\rho} + \frac{2c(1-c)\mathrm{e}_{\mathrm{c}\rho}\mathrm{e}_{\mathrm{cc}}((1-2c)+\mathscr{Y})}{[\mathrm{e}_{\mathrm{cc}}(1-c) - a_{1,2}^2]^2} \pm \vartheta_4 \frac{(1-2c)-\mathscr{Y}}{a_{1,2}}$$

The eigenvalues are all real and the eigenvectors $\mathscr{K}^{\pm}$ and $\mathscr{K}^{0\pm}$ form a complete set of linearly independent eigenvectors. Thus, we have proved that the one-dimensional conservative two-fluid model is hyperbolic and hyperbolicity remains a property of the conservative two-fluid model for more general equations of state.

Finally, the basic structure of the solution of the Riemann problem as a set of elementary waves can be described as follows; from the eigenvalues (20)–(24) we obtain

$$\lim_{u_{\mathrm{r}}\to 0} \nabla\lambda_{\pm}(\mathbb{W}) = \left[\pm\frac{\partial a_{1,2}}{\partial \rho} + \frac{\partial \mathscr{Y}}{\partial \rho}\, u_{\mathrm{r}}, 1, \pm\frac{\partial a_{1,2}}{\partial c} + \frac{\partial \mathscr{Y}}{\partial \rho}\, u_{\mathrm{r}}, \mathscr{Y}\right] \tag{27}$$

$$\lim_{u_{\mathrm{r}}\to 0} \nabla\lambda_{0\pm}(\mathbb{W}) = [0, 0] \tag{28}$$

DOI: 10.1002/fld

So that

$$\lim_{u_r\to 0} \nabla\lambda_{\pm}(\mathbb{W})\cdot\mathscr{K}^{\pm}(\mathbb{W}) = k\left[\pm\frac{\partial a_{1,2}}{\partial\rho} + \frac{\partial\mathscr{Y}}{\partial\rho}\,u_r + (\vartheta_0+\vartheta_1 u_r) + \left(\frac{\partial a_{1,2}}{\partial c} + \frac{\partial\mathscr{Y}}{\partial\rho}\,u_r\right)\vartheta_2 \right.$$
$$\left. \pm\,\vartheta_3\frac{\partial\mathscr{Y}}{\partial c}\,u_r + (\vartheta_4+\vartheta_5 u_r)\mathscr{Y}\right] \neq 0 \tag{29}$$

$$\lim_{u_r\to 0} \nabla\lambda_{0\pm}(\mathbb{W})\cdot\mathscr{K}^{0\pm}(\mathbb{W}) = 0 \tag{30}$$

Thus, the characteristic fields up to first order in u_r associated with the eigenvalues $\lambda_j(\mathbb{W})$, $j = 1, 2, 5, 6$ are genuinely non-linear while those associated with $\lambda_j(\mathbb{W})$, $j = 3, 4$, are linearly degenerate. Having established formally this mathematical foundation, a sufficient framework has been laid for the numerical study based on the Riemann problem. Many modern computational methods use approximate Riemann solutions in algorithms to enhance accuracy of numerical solution. In the next section we provide the necessary ingredients for such a study.

3. THE NUMERICAL METHOD

The hyperbolic conservative two-fluid model presented in Section 2 is difficult to solve analytically since the model possesses a large number of acoustic and convective waves. In addition the number of equations will depend on the number of waves considered, and the closure laws supplied will typically vary and change the solution. Thus, a small modification of the model, will require us to repeat the mathematical analysis and this does not seem practical. Therefore, it seems unnatural to look for analytical solutions to the model. We must instead consider numerical approximations using modern shock-capturing schemes. The method we will use must be flexible enough to handle the modifications of the model without relying on mathematical results obtained analytically. The numerical method will give further insight into the model and will resolve both rarefaction waves and shocks.

Before presenting our numerical method for the hyperbolic conservative two-fluid model, we review some of the basic theory of Godunov-type numerical schemes [30] based on the centred methods. We discretize the x–t plane by choosing a mesh width Δx and a time step Δt, and we define the mesh size $\Delta x = x_{i+1/2} - x_{i-1/2}$, with $i = 1, \ldots, M$. Thus, for a given cell $I_i = [x_{i-1/2}, x_{i+1/2}]$ the location of cell x_i and the cell boundaries $x_{i-1/2}$, $x_{i+1/2}$ are given by

$$x_{i-1/2} = (i-1)\Delta x, \quad x_i = (i-\tfrac{1}{2})\Delta x, \quad x_{i+1/2} = i\Delta x \tag{31}$$

The time step Δt ($\Delta t = t^{n+1} - t^n$) is calculated as marching in time proceeds and satisfies the condition

$$\Delta t = C\frac{\Delta x}{S_{\max}^{(n)}} \tag{32}$$

where C is the Courant–Friedrichs–Lewy (CFL) number with $0 < C \leqslant 1$ and $S_{\max}^{(n)}$ is the maximum wave speed present throughout the domain at time level n chosen

$$S_{\max}^{(n)} = \max_i\{|\lambda_i|\} \tag{33}$$

where λ_i are eigenvalues corresponding to sound waves.

DOI: 10.1002/fld

In Godunov's methods, the approximate solution $\mathbb{U}^{n+1}$, at time t^{n+1}, is obtained by solving Riemann problems at cell interfaces

$$\mathbb{U}_i^{n+1} = \mathbb{U}_i^n - \frac{\Delta t}{\Delta x}[\mathbb{F}_{i+1/2} - \mathbb{F}_{i-1/2}] \tag{34}$$

where the numerical flux $\mathbb{F}_{i+1/2}$ corresponds to the intercell boundary at $x = x_{i+1/2}$ between i and $i+1$. The Godunov flux $\mathbb{F}_{i+1/2}$ may be defined as the physical flux $\mathbb{F}(\mathbb{U})$ evaluated at the solution $\mathbb{U}_{i+1/2}(\frac{x}{t})$ along t-axis in the local coordinate, that is

$$\mathbb{F}_{i+1/2} = \mathbb{F}(\mathbb{U}_{i+1/2}(0)) \tag{35}$$

which is the exact solution of the Riemann problem

$$\partial_t \mathbb{U} + \partial_x \mathbb{F}(\mathbb{U}) = 0 \tag{36}$$

$$\mathbb{U}(x, t^n) = \begin{cases} \mathbb{U}_{i-1}^n, & x < x_{i-1/2} \\ \mathbb{U}_i^n, & x > x_{i-1/2} \end{cases} \tag{37}$$

In practice, solving the non-linear Riemann problem for the hyperbolic conservative two-fluid model may be difficult and time consuming because it requires some iterations for non-linear equations. This suggests using approximate Riemann solvers to build more efficient Godunov-type numerical methods. One of the more modern approximate Riemann solvers is a TVD-centred scheme such as SLIC scheme. The SLIC scheme is a second-order extension of the FORCE scheme [53, 55]. To solve the non-linear Riemann problem (36) for hyperbolic conservative systems, the SLIC scheme results from replacing the Godunov upwind flux in the MUSCL–Hancock scheme [56] by the FORCE flux. For the set of variables $\mathbb{W}$ in (15), the SLIC scheme uses three steps. We follow the procedures given by Toro [30, 53] to recall these steps:

Step I: Data reconstruction, for a set of constant average data states $\mathbb{W}_i^n$, the reconstruction of piecewise constant data $\mathbb{W}_i^n$ into a piecewise linear distribution of the data is given as

$$\mathbb{W}_i(x) = \mathbb{W}_i^n + (x - x_i)\frac{\Delta_i}{\Delta x}, \quad x \in I_i \tag{38}$$

where $x_i = (i - \frac{1}{2})\Delta x$ is the centre of the computing cells I_i, Δ_i are the slopes of six components for the hyperbolic conservative two-fluid model defined as

$$\Delta_i = \tfrac{1}{2}(1 + \Im)\mathbb{W}_{i-1/2} + \tfrac{1}{2}(1 - \Im)\mathbb{W}_{i+1/2} \tag{39}$$

where the parameter $\Im \in [-1, 1]$ (for the hyperbolic conservative two-fluid model $\Im = 0$) and the average between the intercell slopes is given by

$$\mathbb{W}_{i-1/2} = \mathbb{W}_i - \mathbb{W}_{i-1}, \quad \mathbb{W}_{i+1/2} = \mathbb{W}_{i+1} - \mathbb{W}_i \tag{40}$$

Now the boundary extrapolated values are obtained by setting $x = 0$ and $x = \Delta x$ in (38)

$$\mathbb{W}_i^{\mathscr{L}} = \mathbb{W}_i^n - \tfrac{1}{2}\Delta_i; \quad \mathbb{W}_i^{\mathscr{R}} = \mathbb{W}_i^n + \tfrac{1}{2}\Delta_i \tag{41}$$

which are the values of the vector function (38) at the left and right boundaries of I_i.

DOI: 10.1002/fld

Step II: Evolution of extrapolated values, the boundary extrapolated values $\mathbb{W}_i^{\mathscr{L}}$ and $\mathbb{W}_i^{\mathscr{R}}$ evolved in each cell I_i by a time $t=\frac{1}{2}\Delta t$ in terms of conservative variables according to

$$\overline{\mathbb{U}}_i^{\mathscr{L}} = \mathbb{U}_i^{\mathscr{L}} + \frac{1}{2}\frac{\Delta t}{\Delta x}[\mathbb{F}(\mathbb{W}_i^{\mathscr{L}}) - \mathbb{F}(\mathbb{W}_i^{\mathscr{R}})] \tag{42}$$

$$\overline{\mathbb{U}}_i^{\mathscr{R}} = \mathbb{U}_i^{\mathscr{R}} + \frac{1}{2}\frac{\Delta t}{\Delta x}[\mathbb{F}(\mathbb{W}_i^{\mathscr{L}}) - \mathbb{F}(\mathbb{W}_i^{\mathscr{R}})] \tag{43}$$

where $\mathbb{U}_i^{\mathscr{L}}$ and $\mathbb{U}_i^{\mathscr{R}}$ are computed from the boundary extrapolated variables $\mathbb{W}_i^{\mathscr{L}}$ and $\mathbb{W}_i^{\mathscr{R}}$.

Step III: The Riemann problem, we solve the conventional, piecewise constant data Riemann problem for the hyperbolic conservative two-fluid model with initial data

$$\mathbb{W}_{\mathscr{L}} \equiv \overline{\mathbb{U}}_{\mathrm{i}}^{\mathscr{R}}, \quad \mathbb{W}_{\mathscr{R}} \equiv \overline{\mathbb{U}}_{\mathrm{i+1}}^{\mathscr{L}} \tag{44}$$

at each interface $x_{i+1/2}$ to find the similarity solution $\mathbb{W}_{i+1/2}(\frac{x}{t})$.

Now to obtain the Godunov flux (35) at the intercell position $i+1/2$, we evaluate the FORCE flux

$$\mathbb{F}_{i+1/2}^{\mathrm{FORCE}} = \mathbb{F}_{i+1/2}(\overline{\mathbb{U}}_i^{\mathscr{R}}, \overline{\mathbb{U}}_{i+1}^{\mathscr{L}}) = \tfrac{1}{2}(\mathbb{F}_{i+1/2}^{\mathrm{LF}} + \mathbb{F}_{i+1/2}^{\mathrm{RI}}) \tag{45}$$

where $\mathbb{F}_{i+1/2}^{\mathrm{LF}}$ is the Lax–Friedrichs flux given by

$$\mathbb{F}_{i+1/2}^{\mathrm{LF}} = \frac{1}{2}(\mathbb{F}_i^n + \mathbb{F}_{i+1}^n) + \frac{1}{2}\frac{\Delta x}{\Delta t}[\mathbb{U}_i^n - \mathbb{U}_{i+1}^n] \tag{46}$$

and the Richtmyer flux defined as

$$\mathbb{F}_{i+1/2}^{\mathrm{RI}} = \mathbb{F}(\mathbb{U}_{i+1/2}^{\mathrm{RI}}) \tag{47}$$

$$\mathbb{U}_{i+1/2}^{\mathrm{RI}} = \frac{1}{2}(\mathbb{U}_i^n + \mathbb{U}_{i+1}^n) + \frac{1}{2}\frac{\Delta t}{\Delta x}[\mathbb{F}_i^n - \mathbb{F}_{i+1}^n] \tag{48}$$

To avoid the expected spurious oscillations, a TVD constraint is enforced in the data reconstruction step by limiting the slopes Δ_i by $\bar{\Delta}_i$ in (38) with the limited slopes

$$\bar{\Delta}_i = \xi \Delta_i \tag{49}$$

where $\xi = \xi(r)$ is the slope limiter chosen as

$$\xi(r) \begin{cases} = 0, & r \leqslant 0 \\ \leqslant \min\{\xi_{\mathscr{L}}(r), \xi_{\mathscr{R}}(r)\}, & r > 0 \end{cases} \tag{50}$$

where

$$\begin{aligned} \xi_{\mathscr{L}}(r) &= \frac{2\beta_{i-1/2} r}{1 - \Im + (1+\Im) r} \\ \xi_{\mathscr{R}}(r) &= \frac{2\beta_{i+1/2}}{1 - \Im + (1+\Im) r} \\ r &= \frac{\Delta_{i-1/2}}{\Delta_{i+1/2}} \end{aligned} \tag{51}$$

DOI: 10.1002/fld

and

$$\beta_{i-1/2}=\frac{2}{1+C}, \quad \beta_{i+1/2}=\frac{2}{1-C} \tag{52}$$

There exists a variety of limiters that can be used to calculate the slopes in the SLIC scheme. We refer to [30] for a detailed description of the available limiters. In this paper we will only use SUPERBEE limiter which is known to be overcompressive. For limiting values of $\beta_{i-1/2}$ and $\beta_{i+1/2}$ one may eliminate the dependence on C and setting $\beta_{i-1/2}=1=\beta_{i+1/2}$ in (51) to obtain a slope limiter that is similar to the SUPERBEE flux limiter given by

$$\xi_{\rm sb}(r)=\begin{cases} 0 & \text{if } r\leqslant 0 \\ 2r & \text{if } 0\leqslant r\leqslant \frac{1}{2} \\ 1 & \text{if } \frac{1}{2}\leqslant r\leqslant 1 \\ \min\{r, \xi_{\mathscr{R}}(r), 2\} & \text{if } r\geqslant 1 \end{cases} \tag{53}$$

4. TEST PROBLEMS AND NUMERICAL RESULTS

In this section we present and discuss seven numerical test problems. The main purpose is to illustrate the capabilities of the numerical method to capture pressure wave propagation in two and three dimension and to present a suite of one-dimensional test problems for the hyperbolic conservative two-fluid model. In the first test problem, we consider an air–water mixture collision which consists of a symmetric Riemann problem. In the second test problem, we present a grid convergence study for the solution of the Riemann problem obtained in Test 1. In the third test we consider pressure wave propagation for a constructed case and examine the effect of the initial data mixture velocity on the behaviour of these waves. In the fourth test problem, we consider a relaxation of volume concentration to study the effect of this relaxation on the air–water mixture collision. In the fifth test problem we consider additionally an interfacial friction source term in the air–water mixture collision. In the sixth test problem we consider a two-phase shock-tube problem which consists of a Riemann problem for the hyperbolic conservative two-fluid model. Finally, in the last test problem we consider a 2-left and 2-right rarefactions and study the symmetric Riemann problem.

The air–water mixture EOS [57] is governed by EOS (10) and determined by the equations of state for the air and water. The air phase is governed by the perfect gas EOS [58, 59]

$$\mathrm{e}_2=\frac{A_2}{\gamma_2-1}\left(\frac{\rho_2}{\rho_2^0}\right)^{\gamma_2-1}\exp\left(\frac{\mathscr{S}}{c_{\rm V}^2}\right) \tag{54}$$

The EOS for water is defined as follows:

$$\mathrm{e}_1=\frac{A_1}{\gamma_1-1}\left(\frac{\rho_1}{\rho_1^0}\right)^{\gamma_1-1}\exp\left(\frac{\mathscr{S}}{c_V^1}\right)+A_0\frac{\rho_1^0}{\rho_1} \tag{55}$$

which is the stiffened gas equation of state written in terms of density and entropy [58, 60]. In all chosen tests, data consists of two constant states $\mathbb{W}_{\mathscr{L}}=[\rho_{\mathscr{L}}, \alpha_{\mathscr{L}}, u_{\mathscr{L}}, c_{\mathscr{L}}, u_{r\mathscr{L}}, \mathscr{S}_{\mathscr{L}}]^{\rm T}$ and

DOI: 10.1002/fld

Table I. Constants for the numerical study of wave propagation in compressible two-phase flow.

Parameters for the liquid and gas phases	
$\gamma_1 = 2.8$	$\gamma_2 = 1.4$
$\rho_1^0 = 10^3\,\mathrm{kg/m^3}$	$\rho_2^0 = 1\,\mathrm{kg/m^3}$
$c_V^1 = 1495\,\mathrm{J/kg\,K}$	$c_V^2 = 720\,\mathrm{J/kg\,K}$
$A_0 = 8.4999 \times 10^5\,\mathrm{m^2/s^2}$	$A_2 = 10^5\,\mathrm{m^2/s^2}$
$A_1 = 8.5 \times 10^5\,\mathrm{m^2/s^2}$	

$\mathbb{W}_{\mathscr{R}} = [\rho_{\mathscr{R}}, \alpha_{\mathscr{R}}, u_{\mathscr{R}}, c_{\mathscr{R}}, u_{r\mathscr{R}}, \mathscr{S}_{\mathscr{R}}]^{\mathrm{T}}$, separated by a discontinuity at a position $x = x_0$ with $\rho_{\mathscr{L}}$ and $\rho_{\mathscr{R}}$ computed by the given pressures $\mathscr{P}_{\mathscr{L}}$ and $\mathscr{P}_{\mathscr{R}}$. The numerical solutions are found in the spatial domain $-10 \leqslant x \leqslant 10$, which is discretized with M computing cells ($M = 100$ or $M = 1000$ for a coarse mesh or a fine mesh, respectively). The Courant number coefficient is $C = 0.9$, boundary conditions are transmissive, $S_{\max}$ is found using the simplified formula (33), the SUPERBEE limiter was used to obtain second-order accuracy in space. The values for the time, pressure, mixture velocity and spatial domain are: $[t] = 10^{-5}$ s, $[\mathscr{P}] = 10^9$ Pa, $[u] = 10^3$ m/s and $[x] = 10^{-2}$ m. The calculation have been carried out using the parameters defined in Table I. The numerical results were then compared with a reference solution obtained using the SLIC scheme with a very fine mesh [54]. In all test cases, as we shall see later, we compare the results with the Lax–Friedrichs method which has much more numerical diffusion than the SLIC scheme.

4.1. Test 1: Air–water mixture collision

The purpose of this first test is to choose the reference solution for the numerical solution with a very fine mesh and compare the numerical scheme described in Section 3 with this reference solution as well as the standard Lax–Friedrichs method on the solution of the Riemann problem for the hyperbolic conservative two-fluid model. The SLIC scheme is second-order accurate in space and time and stable with Courant number c satisfying $|c| \leqslant 1$. According to Godunov's theorem, spurious oscillations may still be produced in the vicinity of strong gradients. The additional implementation of the TVD feature (total variation diminishing) renders the TVD SLIC scheme quite accurate and stable everywhere. Therefore, computational experience [30, 54] suggests that the TVD SLIC scheme with a very fine mesh, $M = 1000$, is the reference solution for the hyperbolic conservative two-fluid model. Thus, in all the test problems we will compare our results with the reference solution. The left and right states for this Riemann problem are: $\mathscr{P}_{\mathscr{L}} = \mathscr{P}_{\mathscr{R}} = 0.1$, $\alpha_{\mathscr{L}} = 0.5 = \alpha_{\mathscr{R}}$, $u_{\mathscr{L}} = 0.4$, $u_{\mathscr{R}} = -0.4$, $u_{r\mathscr{L}} = 0 = u_{r\mathscr{R}}$, $\mathscr{S}_{\mathscr{L}} = 0 = \mathscr{S}_{\mathscr{R}}$ with $c_{\mathscr{L}}$ and $c_{\mathscr{R}}$ being calculated using the following relation:

$$c = \frac{\alpha \rho_2}{\rho}$$

As the data for the pressure is constant on the left and right states since the mixture velocity u is symmetric, this is a symmetric Riemann problem. The solution of the symmetric Riemann problem is schematically depicted in Figure 1, which consists of a symmetric wave pattern about the t-axis. There are six wave families. The outer waves correspond to the non-linear fields associated with the eigenvalues $\lambda_{1,2} = u - a_{1,2} + \mathscr{Y}(a_{1,2})u_{\mathrm{r}} + \mathscr{O}(u_{\mathrm{r}}^2)$ and $\lambda_{5,6} = u + a_{1,2} + \mathscr{Y}(a_{1,2})u_{\mathrm{r}} + \mathscr{O}(u_{\mathrm{r}}^2)$, where

DOI: 10.1002/fld

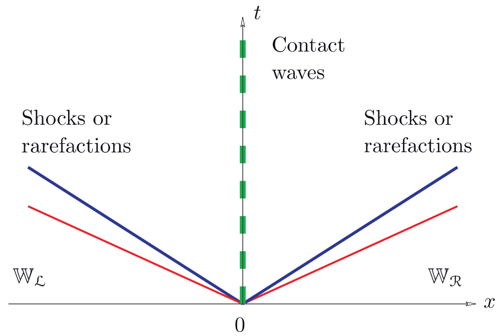

Figure 1. Structure of the exact solution of the symmetric Riemann problem in the x–t plane for the hyperbolic conservative two-fluid model. There are six wave families associated with the eigenvalues (20)–(24).

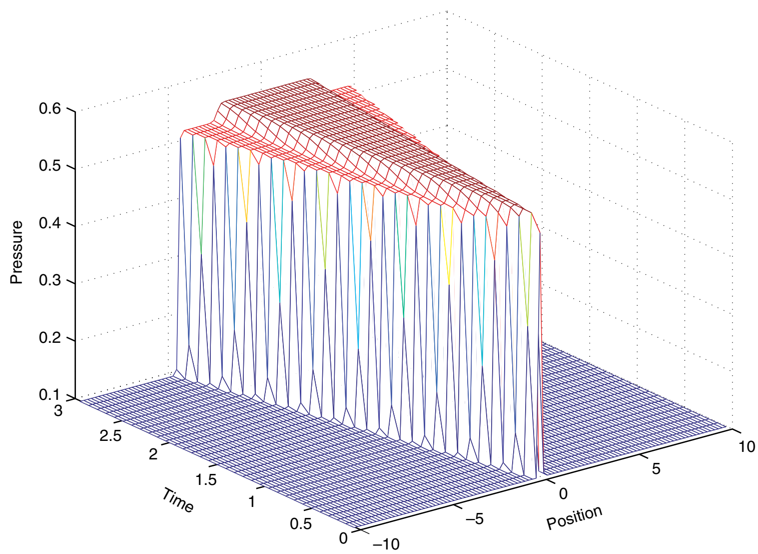

Figure 2. Numerical solution of the Riemann problem. Pressure distribution in three-dimension at $t = 3$.

a_i $(i = 1, 2)$ is the speed of sound of the mixture. The middle wave families correspond to the linearly degenerate fields associated with multiple eigenvalues $\lambda_{3,4} = u$, which in this problem is $\lambda_{3,4} = u = 0$. It is impossible to construct an exact solution for the Riemann problem in a general case. However, for the states $\mathbb{W}_{\mathscr{L}}$ and $\mathbb{W}_{\mathscr{R}}$ we know that the solution is composed of six waves which are either shock, rarefaction or contact discontinuities separated by constant states. Because no analytical solution is available numerical evidence [54] shows that there are four symmetric shock waves travelling in opposite directions that have become shock waves and trivial contact discontinuities centred at $x = x_0 = 0$ as shown in Figures 2 and 3. The benefit of shock wave capturing is more clearly seen in Figure 4 in comparison with Figures 2 and 3. In Figure 4 we give a comparison between the SLIC and Lax–Friedrichs methods for the pressure. In Figure 5 we show the effect of the initial pressure ($\mathscr{P}_{\mathscr{L}} = \mathscr{P}_{\mathscr{R}} = 0.0001, 0.001, 0.1$) on the waves propagation

DOI: 10.1002/fld

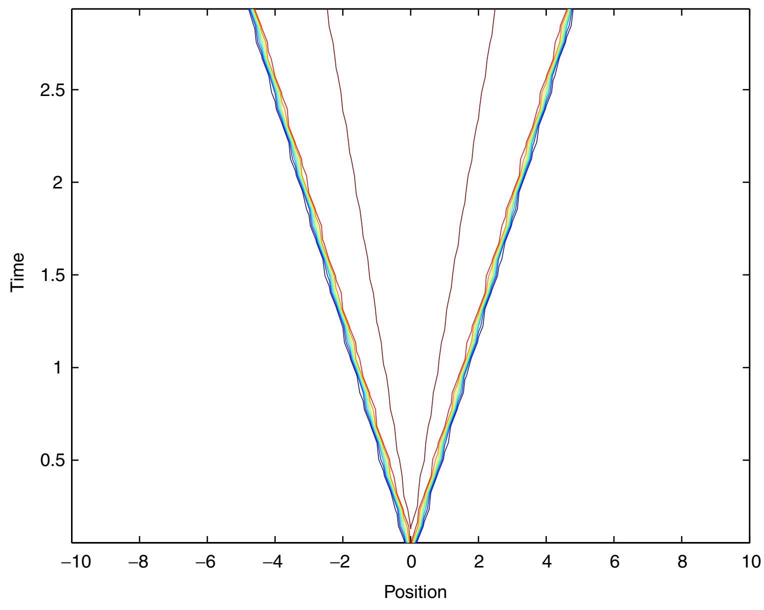

Figure 3. Pressure contours for the Riemann problem at $t = 3$.

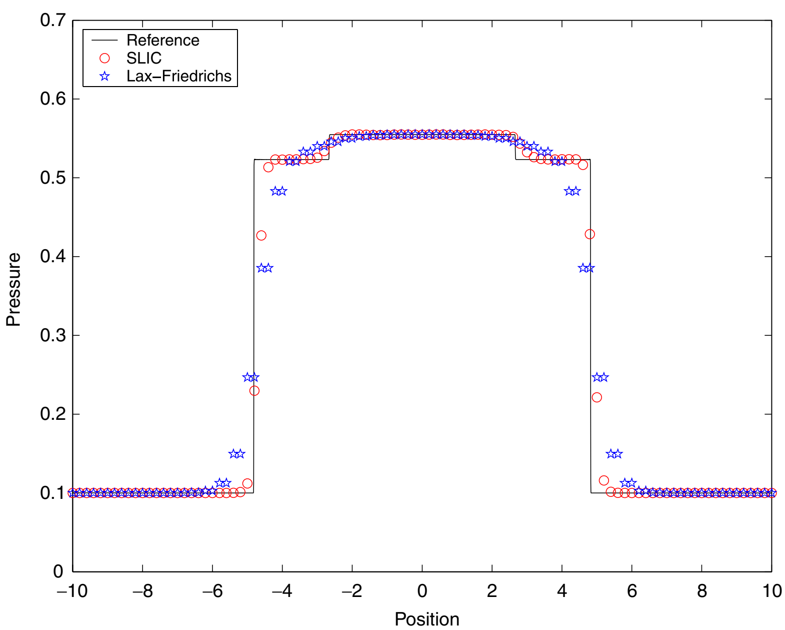

Figure 4. Numerical solution (symbols) for pressure at time 3. SLIC and Lax–Friedrichs methods are compared with the reference solution at 1000 cells.

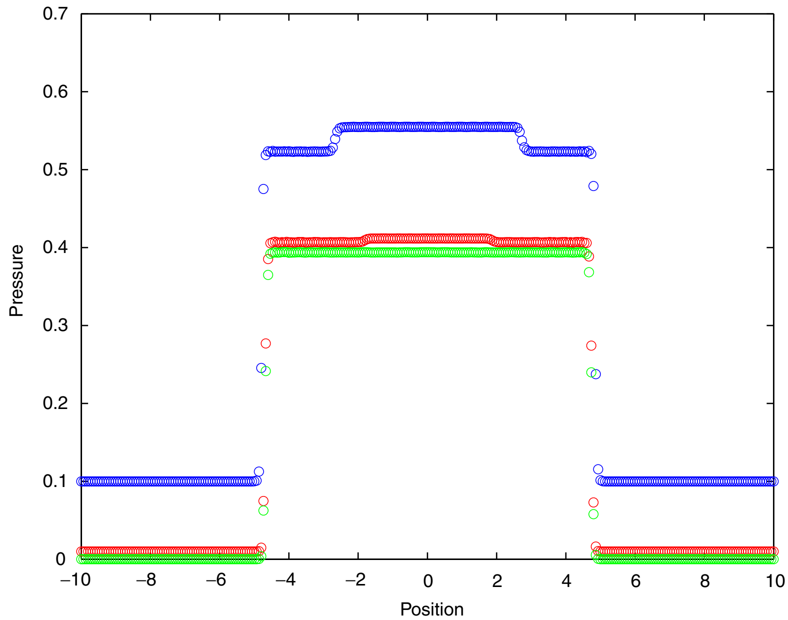

Figure 5. Numerical solution (SLIC scheme). Effect of the initial pressure on the structure of the solution at $t = 3$.

to the left and right after the collision. The increase in the pressure generates a left-going two-shock waves and right-going two-shock as shown in Figure 5.

4.2. Test 2: Grid convergence study

Since no analytical solution is available, a grid convergence study is performed in order to gain some insight into the structure of the solution and to test the convergence and the stability character of SLIC scheme described in Section 3. In this test case the initial conditions for the Riemann problem are chosen as in Test 1. A series of 7 meshes, from 100 to 1000 cells, have been considered in this study. From the results plotted in Figure 6, one can identify a two-shock waves propagating to the far left and to the far right, and a contact wave in the middle of the structure through which the pressure remains constant. An interesting feature of the study shown in Figure 6 is that there are no oscillations at the discontinuity of the pressure when the meshing is refined. This study clearly demonstrate the ability of the SLIC scheme to capture discontinuities.

4.3. Test 3: Pressure wave propagation

Results of the Test 1 show the pressure wave splitting in the two shock waves. The purpose of this test problem is to study the structure of the pressure wave and its dependence on the value of the pressure. Such a problem should be considered by the study of Hugoniot shock conditions; but this problem is a subject of further research. Here we present results of calculations of pressure waves, which satisfy the Hugoniot conditions numerically. To do this we use the values of parameters of state in the star region in the Test 1, which correspond to the values behind the shock wave on the

DOI: 10.1002/fld

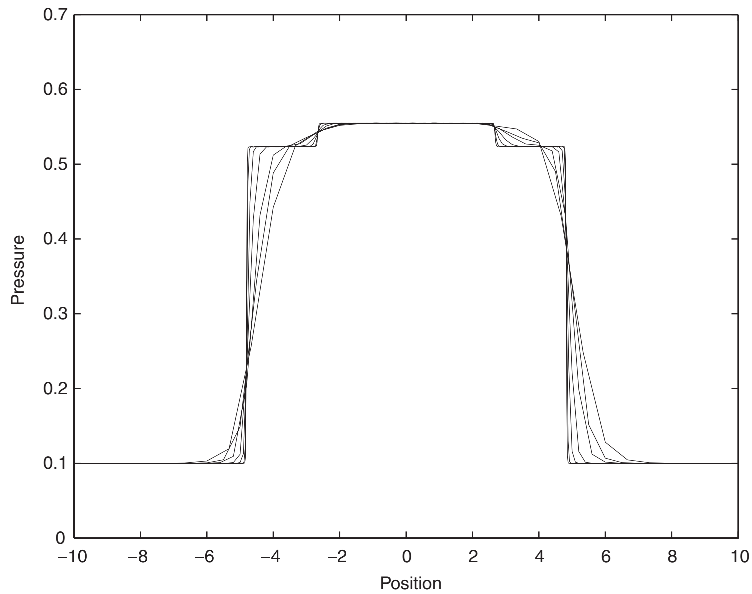

Figure 6. Riemann problem: grid convergence study for the pressure profile with the SLIC scheme at $t = 3$.

Hugoniot curve. We take these values as the initial data on the left side in the Riemann problem. The pressure initial value from the right side is set equal to 0.1. We are interested in simulating a pressure wave generated by increasing the mixture velocity from 0.1 to 0.4 and setting the obtained star states equal to the left data, i.e. $\mathbb{W}^{\star} = \mathbb{W}_{\mathscr{L}}$ in each case of the simulation. If we recall Test 1, we notice that there are right-going two-shock waves in the mixture region (see Figure 4). It is clear that the velocity of the shock waves is equal for all different cases where the mixture velocity increases. The amplitude of the second wave with less velocity increases as the pressure behind the wave becomes stronger. The increase in the mixture velocity generates kinks in the shocks for the pressure solution as shown in Figure 7. These kinks at $u_{\mathscr{R}} = 0.4$ are referred to as 'start-up errors' and were first reported by Woodward and Colella [61]. In addition, a strong two-shocks will form which continue to travel to the right in the mixture two-phase region with reduced mixture velocity as shown in Figure 7. These results were obtained by the SLIC scheme with $M = 300$ cells.

4.4. Test 4: Relaxation of volume concentration

A source term is considered in Test 4 to study the effect of the relaxation of volume concentration on the pressure wave propagation. The source term in the volume concentration equation (4) describes the relaxation of volume concentration to equilibrium state with relaxation time τ; that is the pressures for the phases are equal. In this test problem, the initial conditions are chosen as in Test 1 where pressure is kept constant and equal to 0.1 at the left and right states. For the numerical calculations, the SLIC scheme tested is as explained in Section 3. The results are shown in Figure 8. We have chosen to present plots of the pressure. In Figure 8, it is seen that the effect of τ at $t = 3$ has a decreased amplitude due to the physical attenuation caused by the interphase exchange of volume concentration ($\tau^{-1} = 0.1$, 1.0, 10).

DOI: 10.1002/fld

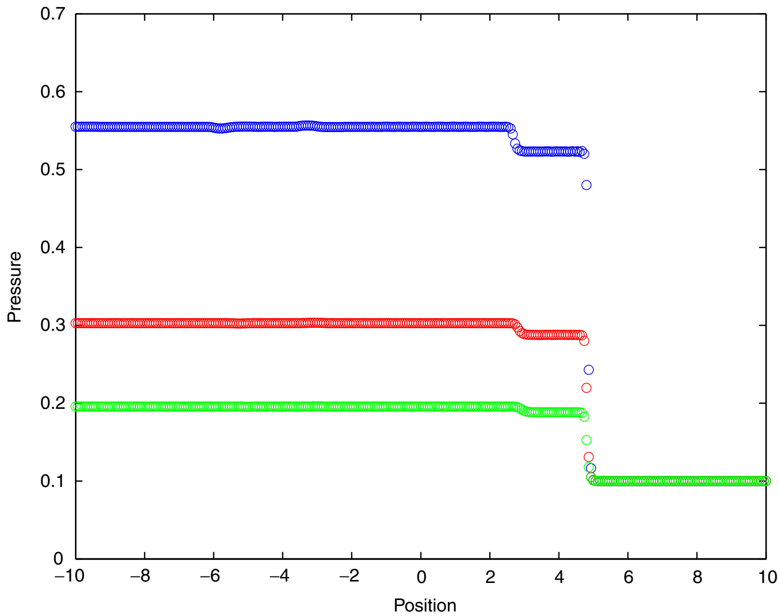

Figure 7. A closer look at the strong 2-shocks propagating to the right obtained with the SLIC scheme at $t = 3$.

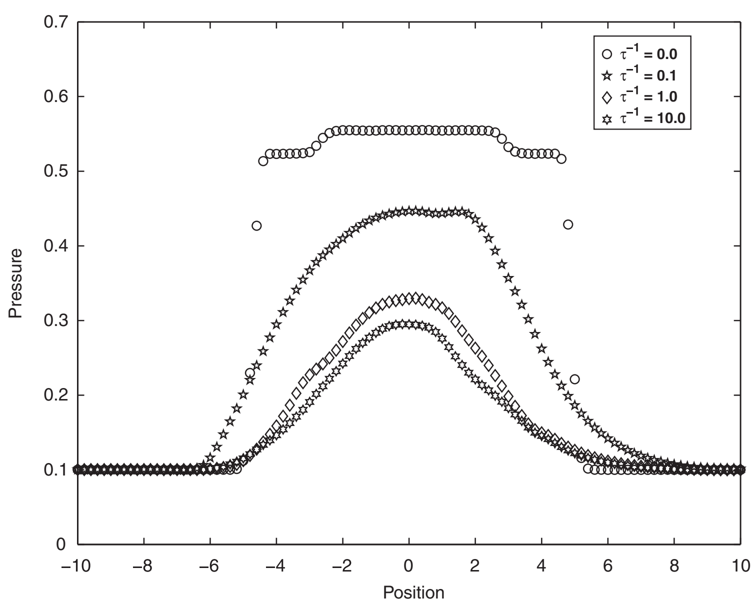

Figure 8. Effect of the relaxation of volume concentration τ on the pressure.

DOI: 10.1002/fld

4.5. Test 5: Effect of volume concentration relaxation and interfacial friction

The purpose of this test problem is to evaluate the capabilities of the SLIC scheme to compute pressure wave propagation with source terms. In this test case we study the effect of the source terms on the hyperbolic conservative two-fluid model. The source terms correspond to the relaxation of volume concentration to equilibrium state with relaxation time τ and to the interfacial friction π as expressed in (8) with κ defined as

$$\kappa = \frac{1}{8} C_{\mathrm{D}} \frac{\rho^2}{\rho_2} |u_{\mathrm{r}}| \tag{56}$$

where the drag coefficient $C_{\mathrm{D}} = 500$, and $\rho_2 = (c\rho)/\alpha$ is the air mass density.

As mentioned before the relaxation of volume concentration and interfacial friction are chiefly responsible for the development of the flow. Three computations were performed on a mesh of 100 cells, using the SLIC scheme, and for three values of $\mathbb{S}(\mathbb{W})$, $\mathbb{S}(\mathbb{W}) = (0, 0, 0, 0, 0, 0)$, $\mathbb{S}(\mathbb{W}) = (0, \phi, 0, 0, \pi, 0)$ and $\mathbb{S}(\mathbb{W}) = (0, \phi, 0, 0, 0, 0)$. Figure 9 shows that the effect of the source terms on the pressure wave propagation is significant.

4.6. Test 6: Mixture two-phase shock-tube problem

We consider a shock tube filled with a water–air mixtures under high pressure at the left and with lower pressure at the right. This test consists of a Riemann problem for the hyperbolic conservative two-fluid model without a source term and with the left and right states defined as

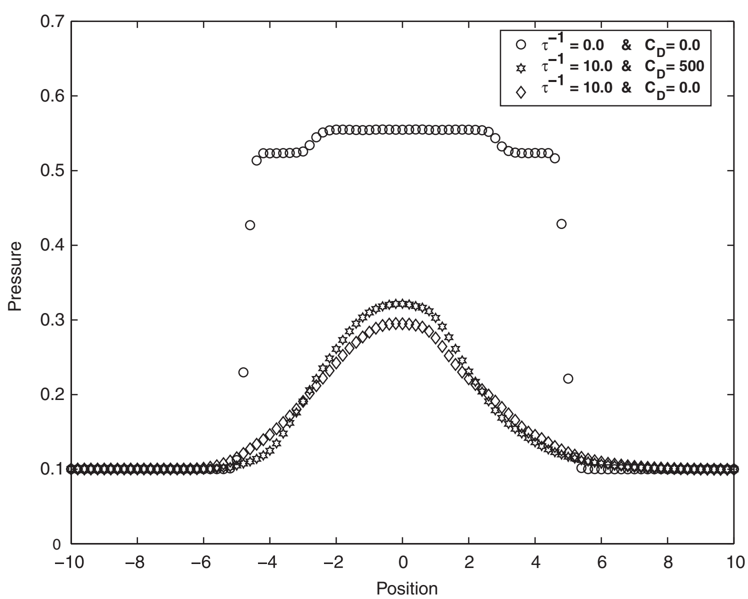

Figure 9. A closer look to the effect of source terms with relaxation time τ and interfacial friction π on structure of the solution of the Riemann problem (pressure).

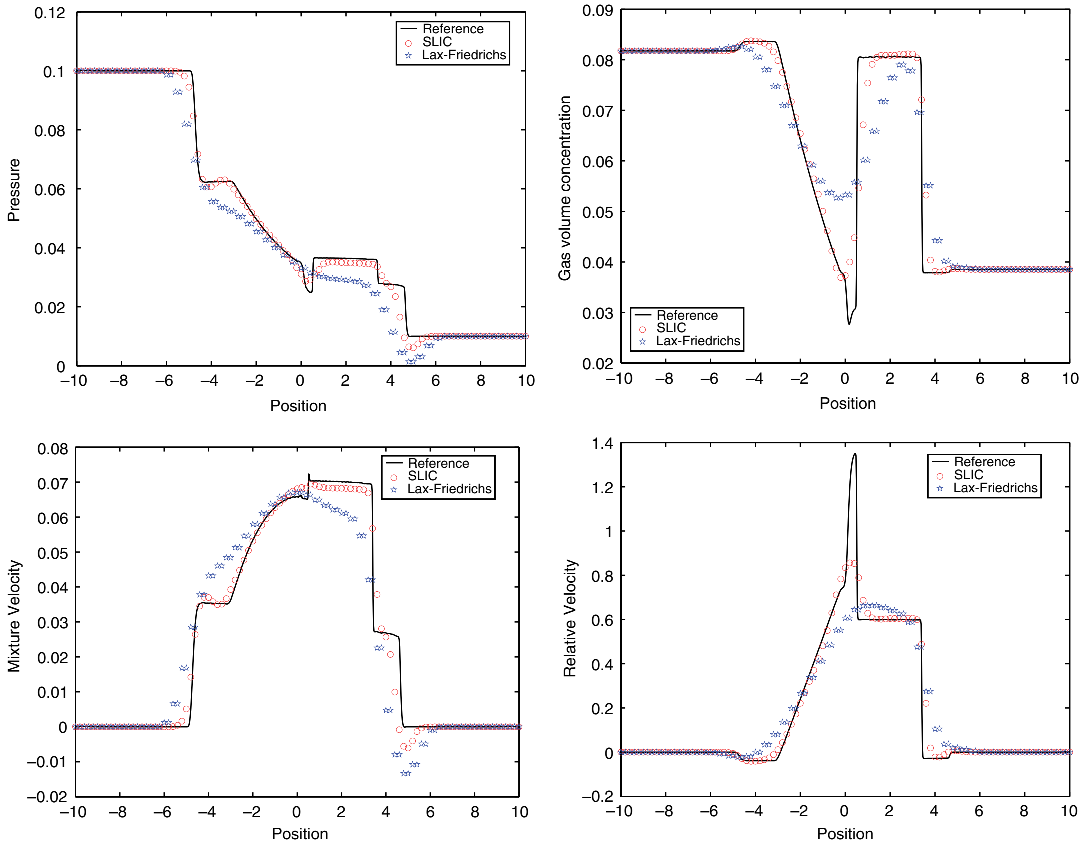

Figure 10. Solution of the Riemann problem for the air–water mixture shock tube. SLIC and Lax–Friedrichs methods (symbols) compared with the reference solution (line) at 1000 cells with $t=3$.

$\mathcal{P}_{\mathcal{L}}=0.1$, $\mathcal{P}_{\mathcal{R}}=0.01$, $\alpha_{\mathcal{L}}=0.4$, $\alpha_{\mathcal{R}}=0.6$, $u_{\mathcal{L}}=u_{\mathcal{R}}=0$, $u_{r\mathcal{L}}=u_{r\mathcal{R}}=0$, $c_{\mathcal{L}}=0.082$, $c_{\mathcal{R}}=0.039$, $\mathcal{S}_{\mathcal{L}}=\mathcal{S}_{\mathcal{R}}=0$. A mesh with 100 cells is used to show the solution numerically. The corresponding results are shown in Figure 10 at time $t=3$. Figure 11 shows results for the same test problem where $\alpha_{\mathcal{L}}=0.0$ and $\alpha_{\mathcal{R}}=1.0$ at time $t=2$.

Bearing in mind that the reference solution is obtained using the SLIC scheme with a very fine mesh [54], the numerical results for the SLIC and Lax–Friedrichs schemes are compared with the reference solution for both test problems. As expected, the SLIC scheme gives a much sharper result of discontinuities compared to the Lax–Friedrichs method.

4.7. Test 7: Four-rarefactions test problem

This test problem consists of a symmetric Riemann problem for the hyperbolic conservative two-fluid model with the left and right states given as $\mathcal{P}_{\mathcal{L}}=0.1=\mathcal{P}_{\mathcal{R}}$, $\alpha_{\mathcal{L}}=0.5$, $\alpha_{\mathcal{R}}=0.5$, $u_{\mathcal{L}}=-0.1$, $u_{\mathcal{R}}=0.1$, $u_{r\mathcal{L}}=u_{r\mathcal{R}}=0$, $c_{\mathcal{L}}=0.1178$, $c_{\mathcal{R}}=0.1178$, $\mathcal{S}_{\mathcal{L}}=\mathcal{S}_{\mathcal{R}}=0$. As previously stated, our

DOI: 10.1002/fld

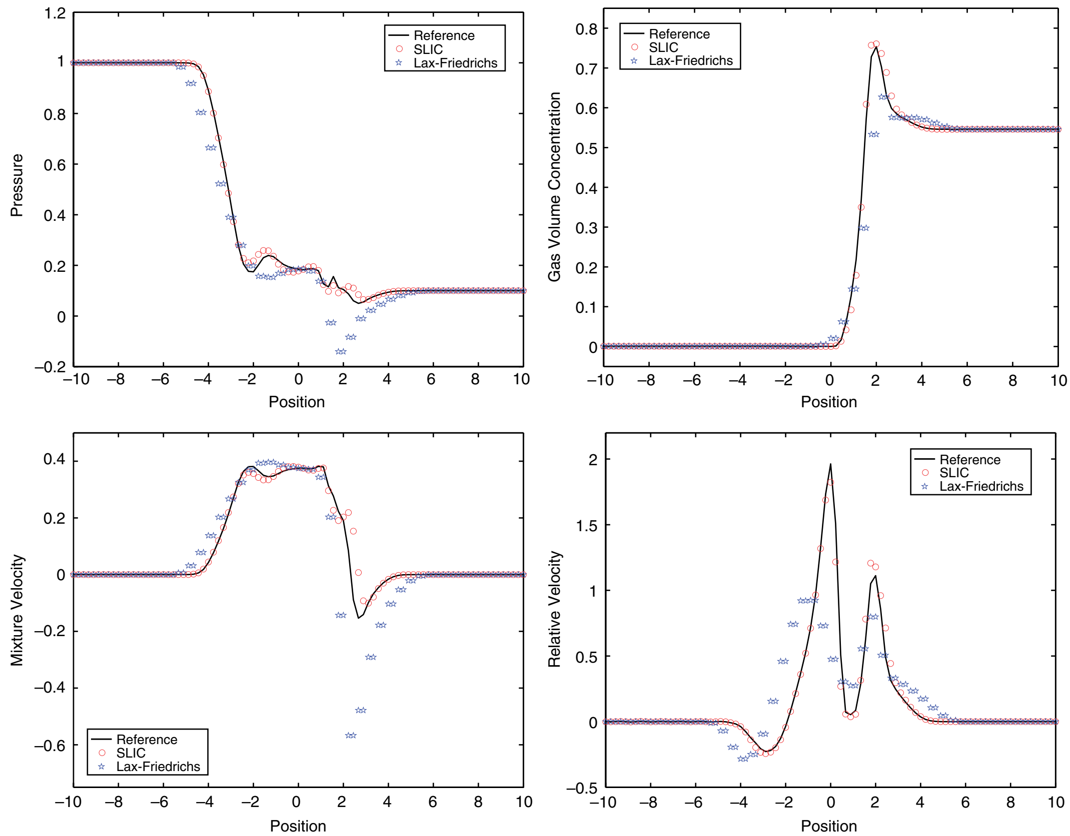

Figure 11. Solution of the Riemann problem for the air–water mixture shock tube. SLIC and Lax–Friedrichs methods (symbols) compared with the reference solution (line) at 1000 cells with $t=2$.

reference solution is a SLIC scheme with a very fine mesh. The numerical solution of the symmetric Riemann problem consists of four symmetric rarefaction waves and a trivial contact discontinuity at $x=x_0=0$. Figure 12 shows a comparison between the SLIC and Lax–Friedrichs methods at time $t=3$. The dip in mixture density and concentration produced in the vicinity of the trivial contact discontinuity is due to spurious mixture density perturbation and well-known anomalies of hyperbolic systems. We do not know or have analytical results for this problem but numerical computations consistently show erroneous solutions for this case. An important conclusion that is valid for this test problem, anticipated from the numerical solution, is that anomalies in the conservative methods deployed here, take the form of a mixture density perturbation in the vicinity of trivial contact discontinuities. Anomalies reported here do affect other hyperbolic systems such as Euler equations, artificial compressibility equations associated with steady incompressible Navier–Stokes equations and equations of Magnetohydrodynamics [62].

DOI: 10.1002/fld

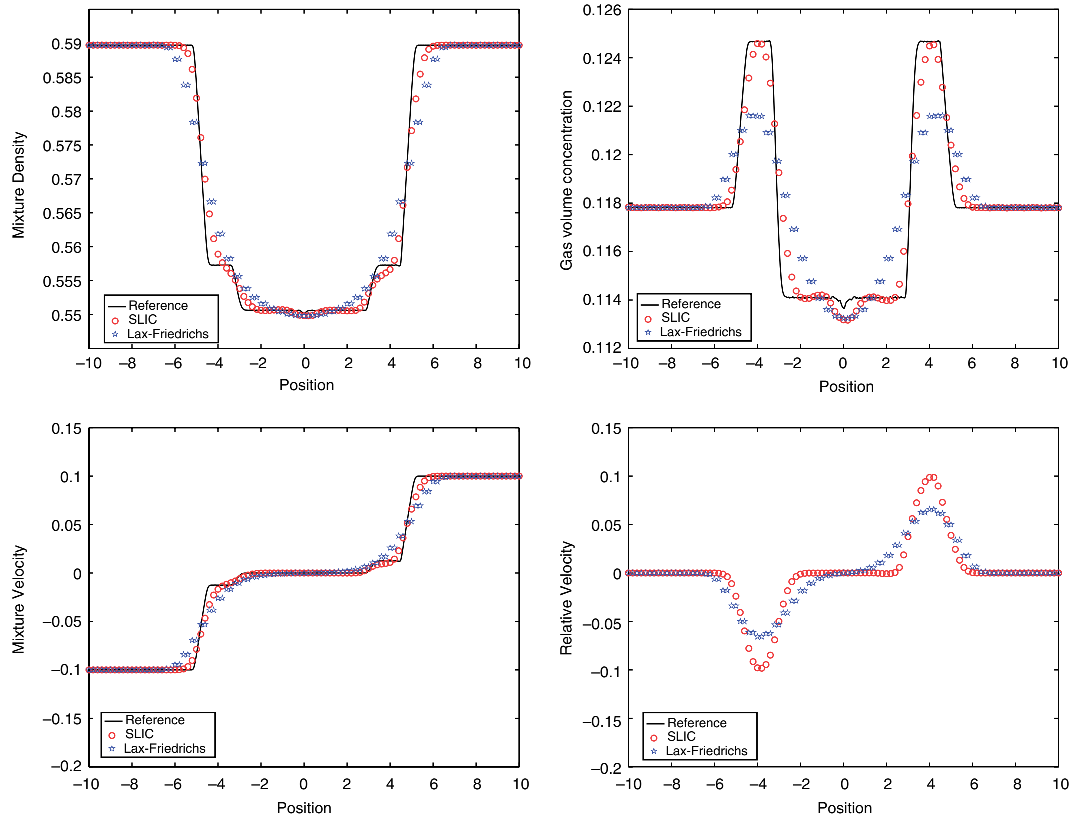

Figure 12. Solution of the Riemann problem for the four rarefaction waves. SLIC and Lax–Friedrichs methods (symbols) compared with the reference solution (line) at 1000 cells with $t = 3$.

5. CONCLUSIONS

In this study, we have examined the mathematical character of a hyperbolic conservative two-phase flow model and issues relevant for the development of a robust numerical solver. The model is based on the extended thermodynamics approach and given by a non-linear symmetric hyperbolic system of partial differential equations written in conservative form. A characteristic analysis reveals that the system of equations is hyperbolic with six real eigenvalues. Through the analysis of the eigenstructure, it is shown that two of the eigenvalues are equal to the mixture velocity whereas the other eigenvalues correspond to the acoustic wave propagation for the mixture. Through a detailed analysis, the derived eigenvectors and the characteristic fields corresponding to the acoustic waves are shown to be genuinely non-linear while the last two are linearly degenerate. Moreover, the model allows the application of modern shock-capturing methods of centred type. Since the model possesses a large number of acoustic waves, it is not easy to upwind all these waves accurately and simply.

We have developed a TVD slope limiter centred scheme SLIC for a wave propagation in compressible two-phase flow model which describes a mixture of air and water. The concept of

DOI: 10.1002/fld

TVD-centred schemes totally avoids the details of the Riemann problem solution. The method developed in this paper can be seen as a formalization of the SLIC scheme suggested by Toro [53] for hyperbolic conservation laws. The centred schemes represent a competitive alternative to the existing upwind schemes for simulating gas–liquid flow. The developed scheme has been applied to the calculation of one-dimensional mixture of air and water two-phase flow to study the Riemann problem numerically. The high-resolution property of the scheme was tested in standard two-phase flow problems. In particular, it has been demonstrated that the SLIC scheme gives a very accurate numerical solution of the wave propagation as demonstrated through the test problems presented in this paper. This is an essential property in order to obtain accurate simulation of gas–liquid flow. In these test problems the source terms have a strong influence on the solution and therefore the said test problems are an excellent reference to test the stated theory; they are useful in showing the performance of the SLIC scheme under extreme conditions which assure high-quality results under more ordinary circumstances. Numerical results show that the derived SLIC scheme is robust with the ability to capture solutions accurately. Additionally the interest of this paper has been on the development of high-order numerical schemes with a capacity to recognize anomalies of conservative methods for inhomogeneous hyperbolic conservation laws arising in two-phase flow models.

Currently used non-conservative two-phase two-fluid flow models are of importance to industrial applications. The mathematical properties of these models are still poorly developed. Moreover, the governing differential equations are complicated and even ill-posed in some models. This stresses the need to develop new models and to have a variety of numerical schemes to investigate their properties. Overall, in this paper, we have shown that through a deeper understanding of numerical schemes of conservation laws, one can develop models and schemes which reveal an improved performance at dealing with realistic two-phase flow problems.

Ongoing work is to further study and generalize this numerical study to the hyperbolic conservative two-fluid model in a natural way using Riemann solutions. Moreover, further work is planned to extend this study to construct an exact [63] and modern approximate Riemann solvers such as Harten, Lax van Leer and Contact (HLLC) that was developed for the simplified two-fluid model [64] which allows the application of Godunov-type methods of upwind-type such TVD weighted average flux (WAF) scheme which is expected to provide an efficient way to calculate more realistic two-phase flow problems. However, it requires a good understanding of the mathematical properties of the hyperbolic conservative two-fluid model. Even though the analysis has not been carried out, some promising results have been obtained in the one-dimensional case [54]. Also an extension of this study to 2D and 3D two-phase flows would be beneficial as some practical problems cannot always be reduced to one-dimensional simulations (depressurization of 2D and 3D pressure vessels, for instance).

This numerical study seems very promising for the numerical solution of two-phase flows as shown by the numerical results for standard two-phase flow problems. As a conclusion, the SLIC scheme turns out to be a very interesting scheme for more complicated models like the hyperbolic conservative two-fluid model studied in this research.

ACKNOWLEDGEMENTS

The second and the fourth authors of this work have been partially supported by the EU Commission under contract FIKS-CT-2000-00050 within the ASTAR project.

REFERENCES

1. Harlow F, Amsden A. A numerical fluid dynamics calculation method for all flow speeds. *Journal of Computational Physics* 1971; **8**:197–213.
2. Harlow F, Amsden A. Numerical calculation of multiphase fluid flow. *Journal of Computational Physics* 1975; **17**:19–52.
3. Patankar S. *Numerical Heat Transfer and Fluid Flow*. Hemisphere: Washington, DC, 1975.
4. Wallis G. *One-Dimensional Two-Phase Flow*. McGraw-Hill: New York, 1969.
5. Ishii M. *Thermo-Fluid Dynamic Theory of Two-Phase Flow*. Eyrolles: Paris, 1975.
6. Wallis G. Review-theoretical models of gas–liquid flows. *Journal of Fluids Engineering* 1982; **104**:279–283.
7. Stewart H, Wendroff B. Two-phase flow: models and methods. *Journal of Computational Physics* 1984; **56**: 363–409.
8. Lahey R, Cheng L, Drew D, Flaherty E. The effect of virtual mass on the numerical stability of accelerating two-phase flows. *International Journal of Multiphase Flow* 1980; **6**:281–294.
9. Ransom V, Hicks D. Hyperbolic two-pressure models for two-phase flow. *Journal of Computational Physics* 1984; **53**:124–151.
10. Baer M, Nunziato J. A two-phase mixture theory for the deflagration-to-detonation transition (DDT) in reactive granular materials. *International Journal of Multiphase Flow* 1986; **12**:861–889.
11. Abgrall R. How to prevent pressure oscillations in multicomponent flow calculations: a quasi conservative approach. *Journal of Computational Physics* 1996; **125**:150–160.
12. Tang H, Huang D. A second-order accurate capturing scheme for 1D inviscid flows of gas and water with vacuum zones. *Journal of Computational Physics* 1996; **128**:301–318.
13. Toumi I, Kumbaro A. A linearized approximate Riemann solver for a two-fluid model. *Journal of Computational Physics* 1996; **124**:286–303.
14. Pokharna H, Mori M, Ransom V. Regularization of two-phase flow models: a comparison of numerical and differential approaches. *Journal of Computational Physics* 1997; **134**:282–295.
15. Bdzil J, Menikoff R, Son S, Kapila A, Stewart D. Two-phase modeling of deflagration-to-detonation transition in granular materials: a critical examination of modeling issues. *Physics of Fluids* 1999; **11**:378–402.
16. Drew D, Passman S. *Theory of Multicomponent Fluids*. Springer: New York, 1999.
17. Städtke H, Worth B, Franchello G. On the hyperbolic nature of two-phase flow equations: characteristic analysis and related numerical methods. In *Godunov Methods*: *Theory and Applications*, Toro EF (ed.). Kluwer Academic/Plenum Publishers: Dordrecht, New York, 2001; 841–862.
18. Gavrilyuk S, Saurel R. Mathematical and numerical modeling of two-phase compressible flows with micro-inertia. *Journal of Computational Physics* 2002; **175**:326–360.
19. Dorovsky V. Continual theory of filtration. *Soviet Geology and Geophysics* 1989; **30**(7):39–45.
20. Dorovsky V, Perepechko Y. Phenomenological description of two-velocity media with relaxing shear stresses. *Journal of Applied Mechanics and Technical Physics* 1992; **33**(3):403–409.
21. Dorovsky V, Perepechko Y, Romensky E. Godunov's scheme for the analysis of the non-linear wave process in the two-velocity media with elastic interaction. *Advanced in Computational Methods in Fluid Dynamics*, *FED* ASME, vol. 196. 1994; 355–366.
22. Godunov S, Romensky E. Thermodynamics, conservation laws and symmetric forms of differential equations in mechanics of continuous media. *Computational Fluid Dynamic Review*. Wiley: New York, 1995; 19–31.
23. Romensky E. Hyperbolic systems of thermodynamically compatible conservation laws in continuum mechanics. *Mathematical and Computer Modelling* 1998; **28**:115–130.
24. Müller I, Ruggeri T. *Rational Extended Thermodynamics*. Springer: New York, 1998.
25. Romensky E. Thermodynamics and hyperbolic systems of balance laws in continuum mechanics. In *Godunov Methods*: *Theory and Applications*, Toro EF (ed.). Kluwer Academic/Plenum Publishers: Dordrecht, New York, 2001; 745–761.
26. Friedrichs K. Symmetric positive linear differential equations. *Communications on Pure and Applied Mathematics* 1958; **11**:333–418.
27. Dafermos C. *Hyperbolic Conservation Laws in Continuum Physics*. Springer: Berlin, 2000.
28. Okazava N, Unai A. Abstract quasilinear evolution equations in a Hilbert space with applications to symmetric hyperbolic systems. *SUT Journal of Mathematics* 1993; **29**(N2):240–263.
29. Sever M. Estimate of the time rate of entropy dissipation for systems of conservation laws. *Journal of Differential Equations* 1996; **130**:127–141.
30. Toro E. *Riemann Solvers and Numerical Methods for Fluid Dynamics*. Springer: Berlin, 1999.

DOI: 10.1002/fld

31. Toro E. Riemann-problem based techniques for computing reactive two-phase flows. In *Numerical Combustion*, Dervieux A, Larrouturou B (eds). Lecture Notes in Physics, vol. 351. Springer: Berlin, 1989; 427–481.
32. Progress and challenges in CFD methods and algorithms. *Proceedings of AGARD Conference*, Seville, Spain, 2–5 October 1995, AGARD-CP-578.
33. Sainsaulieu L. Finite volume approximation of two-phase fluid flows based on an approximate Roe-type Riemann solver. *Journal of Computational Physics* 1995; **121**:1–28.
34. Cocchi J, Saurel R. A Riemann problem based method for compressible multifluid flows. *Journal of Computational Physics* 1997; **137**:265–298.
35. Saurel R, Abgrall R. A multiphase Godunov method for compressible multi-fluid and multiphase flows. *Journal of Computational Physics* 1999; **150**:425–467.
36. Rider W. Advanced numerical techniques for thermal-hydraulics. *Presented National Heat Transfer Conference*, 1993.
37. Toumi I. An upwind numerical method for two-fluid two-phase flow models. *Nuclear Science and Engineering* 1996; **123**:147–168.
38. Shyue K. A fluid-mixture type algorithm for compressible multicomponent flow with van der Waals equation of state. *Journal of Computational Physics* 1999; **156**:43–88.
39. Toumi I, Kumbaro A, Seignole V, Paillère H. Development of a multi-dimensional upwind solver for two-phase water/steam flows. *8th ICONE*, Baltimore, MD, U.S.A., 2–6 April 2000.
40. Shyue K. A fluid-mixture type algorithm for compressible multicomponent flow with Mie–Grüneisen equation of state. *Journal of Computational Physics* 2001; **171**:678–707.
41. Romate J, Meiring W. Solving a hyperbolic two-phase flow model with flow-dependent slip relation. In *Numerical Methods for Fluid Dynamics*, Morton K, Baines M (eds), vol. V. Clarendon Press: Oxford, 1995; 557–564.
42. Coquel F, El Amine K, Godlewski E, Perthame B, Rascle P. A numerical method using upwind for the resolution of two-phase flows. *Journal of Computational Physics* 1997; **136**:272–288.
43. Romate J. An approximate Riemann solver for a two-phase flow model with numerically given slip relation. *Computers and Fluids* 1998; **27**:445–477.
44. Faille I, Heintzé E. A rough finite volume scheme for modeling two-phase flow in a pipeline. *Computers and Fluids* 1999; **28**:213–241.
45. Harten A. High resolution schemes for hyperbolic conservation laws. *Journal of Computational Physics* 1983; **49**:357–393.
46. LeVeque R. *Numerical Methods for Conservation Laws*. Birkhäuser-Verlag: Basel, 1992.
47. Quirk J. A contribution to the great Riemann solver debate. *International Journal for Numerical Methods in Fluids* 1994; **18**:555–575.
48. Godlewski E, Raviart P. *Numerical Approximation of Hyperbolic Systems of Conservation Laws*. Applied Mathematical Science, vol. 118. Springer: Berlin, 1996.
49. Masella J, Faille I, Gallouët T. On an approximate Godunov scheme. *International Journal of Computational Fluid Dynamics* 1999; **12**:133–149.
50. Fjelde K, Karlsen K. High-resolution hybrid primitive-conservative upwind schemes for the drift flux model. *Computers and Fluids* 2002; **31**(3):335–367.
51. Gascón L, Corberán M. Construction of second-order TVD schemes for nonhomogeneous hyperbolic conservation laws. *Journal of Computational Physics* 2001; **172**:261–297.
52. Hwang Y, Chung N. A fast Godunov method for the water-hammer problem. *International Journal for Numerical Methods in Fluids* 2002; **40**:799–819.
53. Toro E, Billett S. Centred TVD schemes for hyperbolic conservation laws. *IMA Journal of Numerical Analysis* 2000; **20**:47–79.
54. Zeidan D. Mathematical and numerical study of two-phase flow models. *Ph.D. Thesis*, Manchester Metropolitan University, Manchester, U.K., 2003.
55. Toro E. On Glimm-related schemes for conservation laws. *Technical Report MMU-9602*, Department of Mathematics and Physics, Manchester Metropolitan University, U.K., 1996.
56. van Leer B. On the relation between the upwind-differencing scheme of Godunov, Enguist–Osher and Roe. *SIAM Journal on Scientific Computing* 1985; **5**(1):1–20.
57. Romenski E, Zeidan D, Slaouti A, Toro EF. Hyperbolic model for compressible two-phase flow. Submitted.
58. Harlow F, Amsden A. *Fluid Dynamics*, Monograph LA-4700, Los Alamos National Laboratory, Los Alamos, NM, 1971.
59. Mader C. *Numerical Modeling of Detonations*. University of California Press Ltd.: London, England, 1979.

DOI: 10.1002/fld

60. Menikoff R, Plohr B. The Riemann problem for fluid flow of real materials. *Reviews of Modern Physics* 1989; **61**:75–130.
61. Woodward P, Colella P. The numerical simulation of two-dimensional fluid flow with strong shocks. *Journal of Computational Physics* 1984; **54**:115–173.
62. Toro E. Anomalies of conservative methods: analysis, numerical evidence and possible cures. *Computational Fluid Dynamics Journal* 2002; **11**(2):128–143.
63. Zeidan D, Toro E, Slaouti A. On the Riemann problem for a hyperbolic two-phase flow model. *2nd European Multiphase Systems Institute Meeting and 40th European Two-Phase Flow Group Meeting*, Royal Institute of Technology, Stockholm, Sweden, 10–13 June 2002.
64. Zeidan D, Toro E, Slaouti A. Numerical simulation of compressible two-phase flow model based on the Riemann problem. ACOMEN, 2002, Liège University, Belgium, 28–31 May 2002.

DOI: 10.1002/fld